Bogusław WIĘCEK [1], Gilbert DE MEY [2], Maria STRAKOWSKA [3], Vasilis CHATZIATHANASIOU [4], Zbigniew GMYREK [5], Michał STRZELECKI [1], Panagiotis CHATZIPANAGIOTOU [4]
[1] INSTITUTE OF ELECTRONICS, LODZ UNIVERSITY OF TECHNOLOGY, 90-924 Łódź, Wólczańska 211/215 St.
[2] ELIS UNIVERSITY OF GENT, Belgium
[3] FACULTY OF ELECTRICAL, ELECTRONIC, COMPUTER AND CONTROL ENGINEERING, LODZ UNIVERSITY OF TECHNOLOGY, 90-924 Łódź, Wólczańska 211/215 St.
[4] ELECTRICAL AND COMPUTER ENGINEERING FACULTY IN ARISTOTLE UNIVERSITY OF THESSALONICA
[5] INSTITUTE OF MECHATRONICS AND INFORMATION SYSTEMS, LODZ UNIVERSITY OF TECHNOLOGY, 90-924 Łódź, Stefanowskiego 18/22 St.

Various applications of complex thermal impedance for transient and AC heat transfer analysis

Abstract

This paper presents the concept and three practical examples of using complex thermal impedance for characterisation different thermal objects. The first problem describes estimation time shift between power and temperature in electric distribution systems with non-sinusoidal currents. The second example discussed here, shows the estimation of power losses distribution in the magnetic punched ferromagnetic strips. The third application presents the inverse thermal modelling of 3-layer biomedical objects (tissues) to estimate the thermal parameters. More details of the presented problems are in the appropriate papers of the authors referenced here.

Keywords: thermal impedance, Nyquist plot, Laplace transform, heat transfer, IR thermography.

1. Introduction

Thermal impedance (Z_{th}) is often used for characterization of thermal objects. It is an old and relatively simple concept, which is very helpful in many practical applications [1, 2, 5, 6, 7, 10]. For almost every electronic component today, producers provide the measured time-dependent thermal impedance $Z_{th}(t)$ for step power excitation or/and for square wave power with varying duty cycles [1]. Due to the complex geometry of some objects, various power excitations and complicated boundary conditions, the thermal modelling can only be perform using the numerical approaches. It makes the problem of predicting the temperature rise in the thermal systems more difficult. There are another concepts of the thermal characterization of objects using so called structure functions [2]. This concept leads to simplify the interpretation of heat transfer through multilayer structures, and it is widely used in power electronics today.

Our approach is slightly different. One can notice that in the Laplace transform domain the solutions of heat transfer differential equations become easier to solve in many practical cases, or even they have the analytical forms [3-6, 10, 13]. We proposed to analyse either temperature variation or thermal impedance in frequency domain using Laplace transform [7, 8, 9, 10]. The concept is presented in Fig. 1. Definition of complex thermal impedance is presented by eqn. (1). We usually assume that the reference temperature is the ambient one, and since the model is linear we define it as equal to 0. It denotes that we calculate the temperature surplus over the ambient, and at the end of analysis we have to add the ambient temperature to the solution.

$$Z_{th}(s) = \frac{T(s)}{P(s)} \tag{1}$$

where: T is temperature above ambient caused by the power dissipated P.

There is a discussion where one should measure the temperature. Usually, in many practical cases we do not have access to the heat source to measure the temperature there. If we use thermography as a measuring tool, we can get the surface temperature only. In such a case we are dealing with so-called transfer thermal impedance. It can vary with the impedance measured in the heat source [5, 6].

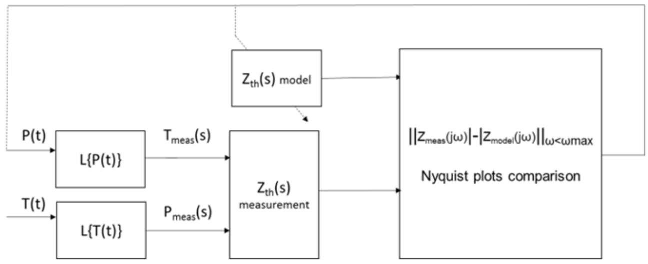

Fig. 1. The proposed methodology of thermal analysis using complex thermal impedance

In addition, we often work with the step power function excitation. It implies $P(s) = P_0/s$ and makes possible to express the complex thermal impedance as $Z_{th}(s)= sT(s)/ P_0$. The very convenient form of thermal impedance, which simplifies the analysis and interpretation, is the Nyquist plot – $\mathrm{Re}\{Z_{th}(j\omega)\} = f(\mathrm{Im}\{Z_{th}(j\omega)\})$.

2. Estimation of temperature increase of energetic cables with non-sinusoidal current

The first practical problem solved using the complex thermal impedance, concerns the estimation of temperature increase in overhead or buried high voltage energetic cables and lines [7]. The problem is important if we take into account the energy losses in the energy distribution system and the safety of system due to the thermal elongation of the overhead cables. In order to evaluate the temperature, at first, the thermal model has to be worked out. Overhead cable is made of aluminium, and it is reinforced by steel – Fig. 2.

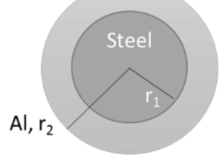

Fig. 2. Cross-section of an overhead cable

Due to the cylindrical symmetry of the cable, 2-D thermal model is expressed by eqns. (2) [7].

$$\begin{aligned} &\lambda_1 \nabla^2 T_1(r) - j\omega C_{v1} T_1(r) = 0 \quad 0 \le r \le r_1 \\ &\lambda_2 \nabla^2 T_2(r) - j\omega C_{v2} T_2(r) = -q \quad r_1 \le r \le r_2 \end{aligned} \tag{2}$$

where λ_i and C_{vi} are the thermal conductivity and volumetric capacity of i-th material, i=1,2, q is the power density in the aluminium layer.

The solution of eqs. (2) uses the Bessel functions [3, 4, 7].

$$T_1(r) = AI_0(\beta_1 r)$$
$$T_2(r) = \frac{q}{j\omega C_{v2}} + BI_0(\beta_2 r) + CK_0(\beta_2 r) \quad (3)$$

where I_0 and K_0 are the zero-th order modified Bessel functions, *A, B, C* are the integration constants that can be determined using the boundary and interface conditions, and

$$\beta_i = \sqrt{\frac{j\omega C_{vi}}{\lambda_i}} \quad (4)$$

Having the temperature distribution (3), one can determine thermal impedance and its Nyquist plot for an overhead cable. For typical energetic cable, one gets: $r_1 = 0.004549$ m, $r_2 = 0.012489$ m, $\lambda_1 = 44.1$ W/m·K, $\lambda_2 = 237$ W/m·K, $C_{v1} = 2.707\cdot10^6$ J/m^{3}K , $C_{v2} = 3.728\cdot10^6$ J/m^{3}K. Modelled Nyguist plot is presented in Fig. 3 [7].

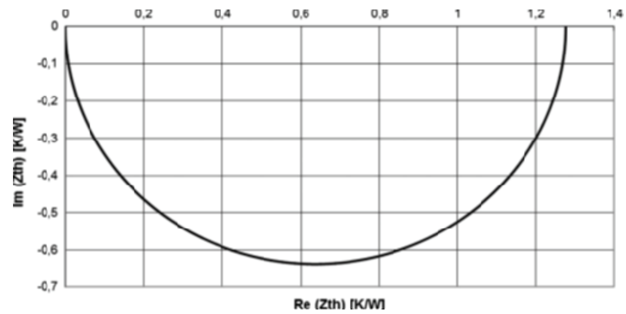

Fig. 3. Nyquist plot of thermal impedance of an overhead cable calculated using the model described above [7]

For the buried underground cable we used a numerical modelling to calculate the thermal impedance because of more complex geometry of the analysed object. Exemplary Nyquist plot of thermal impedance for underground 3-phase line calculated numerically is presented in Fig. 4 [7].

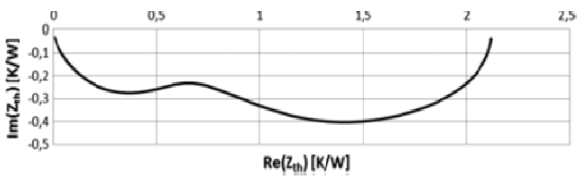

Fig. 4. Nyquist plot of thermal impedance of an underground cable calculated numerically [7]

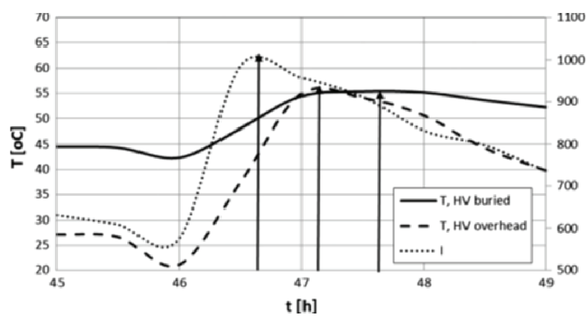

Fig. 5. Peak shift of the current and temperature for overhead and underground cable [7]

Since we have thermal impedance (Nyquist plot), we know the behaviour of the thermal system for different frequencies of the power dissipated in it. This knowledge can be used for estimation the amplitude and the phase shift between the peaks of the current and temperature. Typically, the current is non-sinusoidal containing many harmonic components [7]. We got the current variation for a few months from the electric company for chosen overhead high voltage line. We performed the frequency analysis of the power (current) and temperature using Z_{th} estimated for the data recorded during 1 week. As a result we got the temperature curves versus time, presented in Fig. 5.

The character of variations of temperature, current and power is similar. The temperature delayed in reference to the current by 61.8 min for buried and 28.2 min. for overhead cable [7].

3. Losses in punched ferromagnetic strips

The ferromagnetic strips used for transformers' cores are mechanically or optically cut. During this process the properties of ferromagnetic material significantly change. It results in increasing the power losses in the punched area. The width of this area is typically a few hundreds micrometres [8]. The effect of damage and larger power dissipation can be observed by sensitive infrared system when the magnetic flux affects the strip (Fig. 6). We registered temperature about 0.2 K higher at the point no. 4 in impact region, than at the point no. 1 on another undamaged side of the strip – Fig. 7. We made the experiment with 1.7 T magnetic flux density and measured the transient process of temperature rise after applying the magnetic flux to the sample.

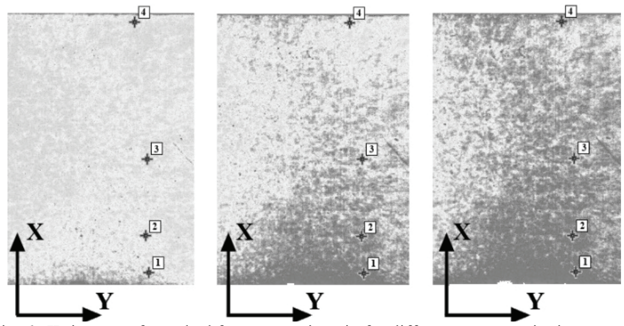

Fig. 6. IR images of punched ferromagnetic strip for different moments in time after start the heating

Temperature curves vs. time were noisy due to its low excess of the temperature, above the ambient. Therefore the exponential approximation were needed as it is shown in Fig. 7.

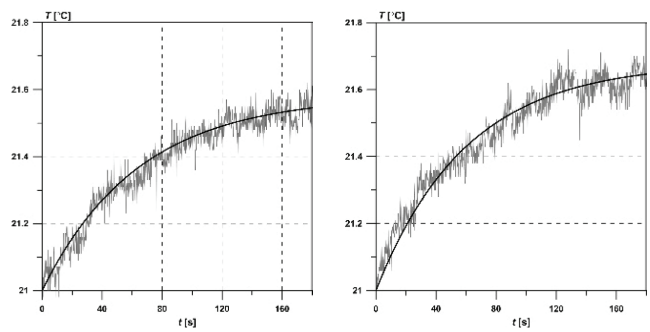

Fig. 7. Temperature rise at points P1 and P4 of the strip, at the distance 1.5 mm and 29.3 mm from the edge (measured using photon IR camera) [8]

In order to calculate the power dissipated in the punched area, a simple thermal model was worked out. The strip of size 30×30 mm was divided into 11 rectangular sectors as shown in Fig. 8. The thickness t_s of the strip was much lower than its length d and the magnetic field was uniformly distributed along the strip width. In consequence 1-D thermal model was used in modelling.

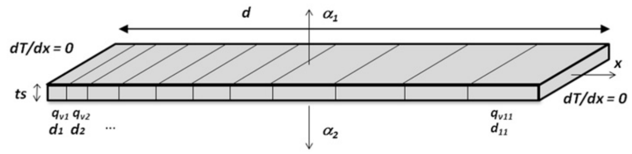

Fig. 8. Sectional model of the magnetic strip [8]

1-D thermal model (5) in Laplace transform domain includes convection cooling along the strip. Convection was modelled using heat transfer coefficient $\alpha = \alpha_1 + \alpha_2$ which was constant but different for both sides of the strip.

$$\lambda \frac{\mathrm{d}^2 T}{\mathrm{d}x^2} - \left(\rho \cdot c_s \cdot s + \frac{\alpha}{t_s}\right) T = -q_{vi}$$

$$\frac{\mathrm{d}^2 T}{\mathrm{d}x^2} - \frac{T}{L^2} = -\frac{q_{vi}}{\lambda} \tag{5}$$

where ρ is material density, c_s is specific heat, λ is thermal conductivity coefficient, t_s is thickness of strip, α is heat transfer coefficients $\alpha = \alpha_1 + \alpha_2$, q_{vi} is the volumetric power density dissipated in each section, i=1..11.

L is so-called diffusion length and it is a complex value given by eqn. (6).

$$L(s) = \frac{1}{\sqrt{\dfrac{\rho \cdot c_s \cdot s}{\lambda} + \dfrac{\alpha}{\lambda t_s}}} \tag{6}$$

The solution of eqn. (5) for each section is analytical, eq. (7).

$$T(s) = A_i(s) \cdot e^{-\frac{x}{L(s)}} + B_i(s) \cdot e^{\frac{x}{L(s)}} + \frac{p_{vi} L^2}{2\lambda} \tag{7}$$

As before the integral constants A_i and B_i were determined using the boundary and interface conditions between the sections [8]. Optimization procedure was used to adapt the power density in each section to fit temperature from the model and measurement at different points of the strip. The calculation was performed for the following material parameters: density ρ = 7850 kg/m^3, thermal conductivity λ = 44.1 W/m·K, specific heat c_s =475 J/kgK, convective heat transfer coefficient α = 25.1 W/m^{2}K. The final result of the power distribution in punched ferromagnetic strip is presented in Fig. 9. The obtained results agree with ones published in the literature [9].

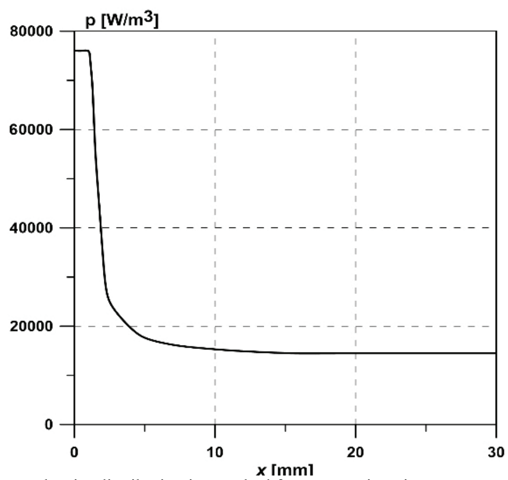

Fig. 9. Power density distribution in punched ferromagnetic strip

4. Thermal modelling multilayers biomedical objects

The aim of the next research was to evaluate the thermal properties of a tissue by inverse thermal modelling [10]. Our hypothesis was that using the thermal parameters of multilayer biomedical structure, it is possible to differentiate the pathological and physiological states of tissue, especially the skin.

We used cold-stress approach. It denotes that we cooled down the skin by a few degrees Celsius to monitor the recovery to the thermal equilibrium. By comparing the temperature rise from the model and measurement we could estimate thermal diffusivity, conductivity and perfusion of each layer of the tissue.

At first the thermal model of 3-layer skin tissue was worked out. The model uses the well-known Pennes equation (8) [11]. It describes bioheat transfer in human tissue with perfusion and metabolism.

$$\rho \cdot c \cdot \frac{\partial T}{\partial t} = \lambda \cdot \frac{\partial^2 T}{\partial x^2} + Q_{per} + Q_{met} \tag{8}$$

where: Q_{per} is the heat corresponding to perfusion, Q_{met} is a constant value heat corresponding to metabolic processes in a tissue. Q_{met} takes values between 245-24500 W/m^3, and was neglected in this research. We assume that the metabolic heat in the skin is rather small.

As before, the thermal model was defined in Laplace transform domain in order to simplify the time dependent, transient calculations, eqns. (9).

$$\begin{aligned} &\lambda \frac{d^2 T}{dx^2} - T(\rho \cdot c_s \cdot s + w \cdot c_b \cdot \rho_b) = 0 \\ &\frac{d^2 T}{dx^2} - \frac{T}{L^2} = 0 \\ &L(s) = \frac{1}{\sqrt{(\rho \cdot c_s \cdot s + w \cdot c_b \cdot \rho_b)/\lambda}} \end{aligned} \tag{9}$$

where: ρ – tissue density (kg/m^3), c_s – specific heat (J/kgK), λ – thermal conductivity (W/m·K), w – perfusion coefficient (1/s), L – thermal diffusion length (m).

First step of the measurement procedure was to cool down the part of the body by a cooling gel. Then we took off the cooling gel and started the measurement. One assumed that the thermal excitation was the unit step function. We looked for thermal response in Laplace transform domain. Either cooling or heating by the convection from the ambient was taken into account by the boundary condition [10]. 1-D heat transfer model of a human tissue is sufficient for this problem. One has to underline that each layer of multilayer structure has its own solutions of eqs. (9). Then, the interface conditions integrate the solution for the whole structure. One assumes the continuity of the heat fluxes and temperature at the interfaces between the layers. As final result, the model provides temperature variation on the upper surface in order to compare it with the thermographic measurement [10, 12, 13].

The overall procedure consists of:

- measurement of temperature after release the cold stress,
- approximation of temperature recovery to reduce the noise [10], Fig. 10,
- thermal modelling in Laplace transform domain,
- finding Z_{th} from the model and measurement,
- optimisation – adapting values of thermal parameters and/or power to match temperature from the model and measurement in the frequency domain – Fig. 11, Table 1.

Approximation of temperature curve obtained from the thermographic measurements was performed using combination of exponential and *erfc* functions. Such an approximation gives a necessary smoothing, and it has the analytical form of Laplace transform [10]. It simplifies the calculations and makes them much faster.

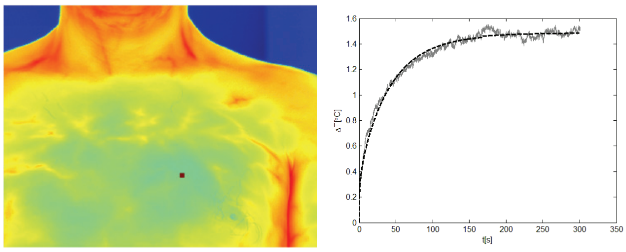

Fig. 10. Thermography image and temperature evolution vs. time in the chosen point on the chest after cold provocation [10]

A program in MATLAB environment was prepared to implement the entire method. The main window of this program is in Fig. 11 presented. In Fig. 11 and Table 1, there are results of the optimisation procedure, that allowed estimating the values of thermal parameters of the multilayer skin structure.

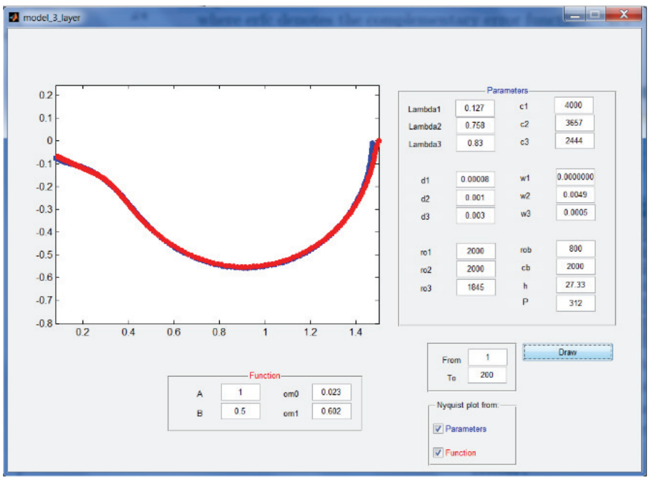

Fig. 11. Thermal impedance comparison for 1-D thermal model and measurement

We believe that our methodology of thermal investigations will allow to diagnose the pathologies of the skin, such as psoriasis, melanoma, allergy, etc.

Tab. 1. Thermal parameters of the human skin obtained using inverse thermal model [10]

	Layer 1 epidermis	Layer 2 dermis	Layer 3 hypodermis	Blood
Thermal conductivity K, W/m·K	0.127	0.758	0.83	-
Thickness d, mm	0.08	1	3	-
Density ρ, kg/m^3	2000	2000	1845	800
Specific heat c, J/kgK	4000	3657	2444	2000
Perfusion W, 1/s	$1.01\cdot10^{-8}$	0.0049	0.0005	-

5. Conclusions

Three different applications of thermal modelling in Laplace transform domain leading to the determination of complex thermal impedance were presented in this paper. All of them confirm the usefulness and simplicity of applying Z_{th} for 1-D and 2-D transient or AC modelling of heat transfer in various object. Moreover this modelling is partly analytical. It makes the entire methodology faster in operation and allows the better physical understanding the thermal processes and heat transfer in complex objects. If necessary, our approach of forward and inverse thermal modelling can be extended by using full numerical solvers of heat transfer differential equations. It can be required if the objects have the complicated structure, are nonlinear, or there are time or temperature dependent boundary conditions.

6. References

[1] Thermal Resistance Theory and Practice, Special Subject Book, Infineon Technologies, January 2000, http://www.infineon.com
[2] Szekely V.: Identification of RC Networks by Deconvolution: Chances and Limits, IEEE Transaction on Circuits and Systems-I. Theory and Applications, Vol.45, No.3, March 1998, pp. 244-258.
[3] Bejan A. Heat transfer. New York: Wiley; 1992.
[4] Incropera F, DeWitt D.: Introduction to heat transfer. New York: Wiley; 1985.
[5] Vermeersch B., De Mey G.: Thermal impedance plots of micro scaled devices. Microelectron Reliab. 2006, vol.46, pp.174-177.
[6] Vermeersch B., De Mey G.: Influence of substrate thickness on thermal impedance of microelectronic structures. Microelectron. Reliab. 2007, vol 47, pp.437-443.
[7] Wiecek B., De Mey G. Chatziathanasiou V., Papagiannakis A., Theodosoglou I.: Harmonic analysis of dynamic thermal problems in high voltage overhead transmission lines and buried cables. Electrical Power and Energy Systems 58 (2014) , pp. 199–205.
[8] Gmyrek Z., Strakowska M., Wiecek B.: A method of local magnetic loss determination in punched ferromagnetic strips. Journal of Magnetism and Magnetic Materials, vol. 355, 2014, pp. 282-288.
[9] Baudouin P., Houbaert Y., Tumanski S.: Journal of Magnetism and Magnetic Materials, 254-255 (2003), 32-35.
[10] Strakowska M., De Mey G., Wiecek B., Strzelecki M.: A Three Layer Model for The Thermal Impedance of the Human Skin: Modeling and Experimental Measurements, Journal of Mechanics in Medicine and Biology. Vol. 15, No. 3 (2015) 1550044 (11 pages), in press.
[11] Pennes H. H.: Analysis of Tissue and Arterial Blood Temperatures in the Resting Forearm. Journal of Applied Physiology, 1: 93-122, 1948, ISSN 1522-1601.
[12] Laaperi E., Laaperi A., Strakowska M., Wiecek B., Przymusiala. P.: Cold provocation improves breast cancer detection with IR thermography - a pilot study. Thermology International, 22: 152-156, 2012.
[13] Wiecek B., Strakowska M., De Mey G., et al.: Influence of Infrared Radiation on the Human Skin Temperature - Experimental Data and Modelling, 13(3): J. Mech. Med. Biol. 13(3): 1350025-1-10, 2013.

Received: 12.03.2015 *Paper reviewed* *Accepted: 05.05.2015*

Prof. Bogusław WIĘCEK

Bogusław Więcek is the head of Electronic Circuit and Thermography Division in Institute of Electronics where he has worked for more than 35 years. Actually, he is the co-author of 68 papers on JCR list. He was the supervisor of 9 finished Ph.D. processes. His scientific interests are: industrial and biomedical applications of IR thermography, heat transfer modelling and advanced IR analog and digital system developments.

e-mail: wiecek@p.lodz.pl

Prof. Gilbert DE MEY

Gilbert De Mey was graduated at University of Ghent, where he is now a professor. He conducts research on thermal problems in electronic systems. The main area of the research regards problems of heat exchange in electronic components and systems. It includes theoretical modeling and studies on heat transfer by convection and radiation.

e-mail: gilbert.demey@ugent.be

M.Sc. Maria STRĄKOWSKA

She graduated from the Faculty of Electrical, Electronic, Computer and Control Engineering Lodz University of Technology, majoring in Electronics and Telecommunications, specialty Images and Signal Processing. In 2010, she began doctoral studies. Her research interests focus around the thermographic image measurement and processing as well as the modeling of thermal phenomena for biomedical applications.

e-mail: maria.strakowska@dokt.p.lodz.pl

Prof. Vasilis CHATZIATHANASIOU

Prof. Vasilis Chatziathanasiou was graduated from Electrical and Computer Engineering Faculty in Aristotle University of Thessalonica in Greece. He is now the professor there. His scientific interests are in the domain of coupled electrothermal problems in power transmission and distribution systems.

e-mail: hatziath@eng.auth.gr

Prof. Zbigniew GMYREK

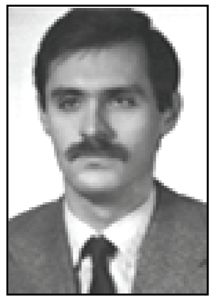

Prof. Zbigniew Gmyrek works as the professor at Lodz University of Technology. He is the co-author of more than 100 papers. He is the reviewer for various journals, e.g.: IEEE Transaction on Industrial Electronics, IEEE Transaction on Industry Applications and many international conferences, such as: ICEM, ECCE, ISIE, INTERMAG. His scientific interest is the measurement and modelling of magnetic material used for electrical machines and apparatus.

e-mail: zbigniew.gmyrek@p.lodz.pl

Prof. Michał STRZELECKI

Professor Michal Strzelecki is at the Technical University of Lodz in Biomedical Engineering Division, Institute of Electronics. Currently, he is a Deputy Director of the Institute of Electronics. His research interests covers artificial intelligence, image processing and analysis, especially biomedical image texture segmentation, pattern recognition. He is an author or co-author of more than 200 scientific publications. Prof. Strzelecki is a member of Association for Image Processing and Polish Society of Medical Informatics.

e-mail: michal.strzelecki@p.lodz.pl

Dipl. Eng. Panagiotis CHATZIPANAGIOTOU

Dipl. Eng. Panagiotis Chatzipanagiotou received the Diploma degree in Electrical and Computer Engineering from the Aristotle University of Thessaloniki, Greece in 2012, where he is pursuing the Ph.D in Electrical Engineering since February 2013. His research interests lie in the field of thermal characterization of power lines and cables.

e-mail: chatzipa@auth.gr